Langmuir

Article

pubs.acs.org/Langmuir

Photovoltaic Hybrid Films with Polythiophene Growing on Monoclinic WO_3 Semiconductor Substrates

Zhouyong Yang and Xiuyuan Ni*

State Key Laboratory of Molecular Engineering of Polymer, Department of Macromolecular Science, Fudan University, Shanghai 200433, People's Republic of China

Supporting Information

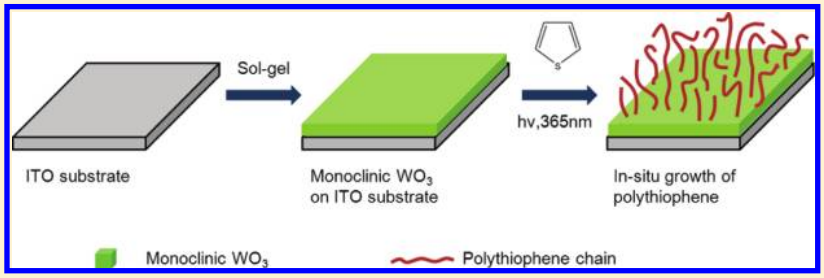

ABSTRACT: A new photovoltaic film consisting of monoclinic WO_3 semiconductor and conjugated polythiophene (PT) is prepared via an in situ polymerization which is initiated by photoexcited WO_3. It is observed that PT grows on the WO_3 substrate along with reaction time, leading to uniform and high quality PT-WO_3 composite films. Structures of the as-synthesized films are studied by using Raman and X-ray photoelectron spectroscopy (XPS) with the aim of gaining an insight into the interface. The results show that the sulfur sites of PT are bound to the semiconductor through a strong linkage and an acceptor−donor complex is formed as a result of the electron transfer from PT to WO_3. The cyclic voltammetry analysis confirms the charge-transfer reaction. Film devices are fabricated by using the PT-WO_3 composite film as the active layer and measured under AM 1.5G illumination for the photocurrents and incident photon-to-current conversion efficiency.

INTRODUCTION

The photovoltaic devices which adopt π-conjugated polymers to sensitize nanocrystal semiconductors promise to provide a low-cost alternative to traditional silicon solar cells and dye-sensitized cells.[1−5] The film-forming capacity of the polymers makes possible the fabrication of large-area and flexible thin-film devices. The target to produce efficient solar cells asks the hybrid polymer/nanocrystals composite, which serves as the active layer, to meet various physical and chemical demands.[3−5] The interface between the polymer and nanocrystals is one of major factors to determine the photovoltaic performance through affecting the charge dissociation.[3−5] An efficient charge-dissociation may need intimate interfaces, in which a covalent linkage makes possible the intramolecular transfer. However, strategies for obtaining stabilized-interface photovoltaic composites are still a challenge because the original π-conjugated polymers lack an anchoring group on the surface of the semiconductors. If conventional deposition techniques such as spin-coating and screen-printing are employed,[6] then the conjugated polymers are weakly adsorbed by the nanocrystals in the composites. A promising strategy is to graft the conjugated polymers onto the semiconductors through a Heck coupling step.[7,8] Moreover, functionalizing the polymers with suitable groups (e.g., cyano and amino) also brings the polymers into an intimate contact with the nanocrystals.[9] With those modifications, the electron transfer and energy conversion is improved.[7−9] Our previous studies have provided an efficient route to synthesize the hybrid composites, by using photoexcited-nanocrystals to initiate polymerizations.[10] We have immediately obtained a composite containing the conjugated polymer and nanocrystals once the polymerization was accomplished. Thereafter, several important materials including the photovoltaic polypyrrole-TiO_2 composite, photoconductive PVK-ZnO material, and water-soluble fluorescent ZnS quantum dots have been synthesized.[11−13] Mechanism investigations have correlated the initiation reactions to the photogenerated holes that are trapped at the surface of semiconductors.[10]

Recently, the polymer photovoltaic devices have been improved to exhibit remarkable efficiencies by tailoring the device structures to electrons and holes transfer.[14] Despite the obvious effects arising from the incorporated hole-extracting layer and buffer layer,[15] the active-layer still plays an important role of deciding the photovoltaic tendency of the device.[16] The active layers pertaining to the polymer photovoltaic devices, in fact, are confined to limited components. Most of the studies have used the nanocrystal TiO_2, ZnO and CdSe semiconductors to suite the electronic properties of conjugated poly(3-hexylthiophene) (P3HT), phenylene vinylene (PPV), and poly(3-octylthiophene) (P3OT) derivatives polymers.[17]

Received: December 18, 2011
Revised: February 10, 2012
Published: February 15, 2012

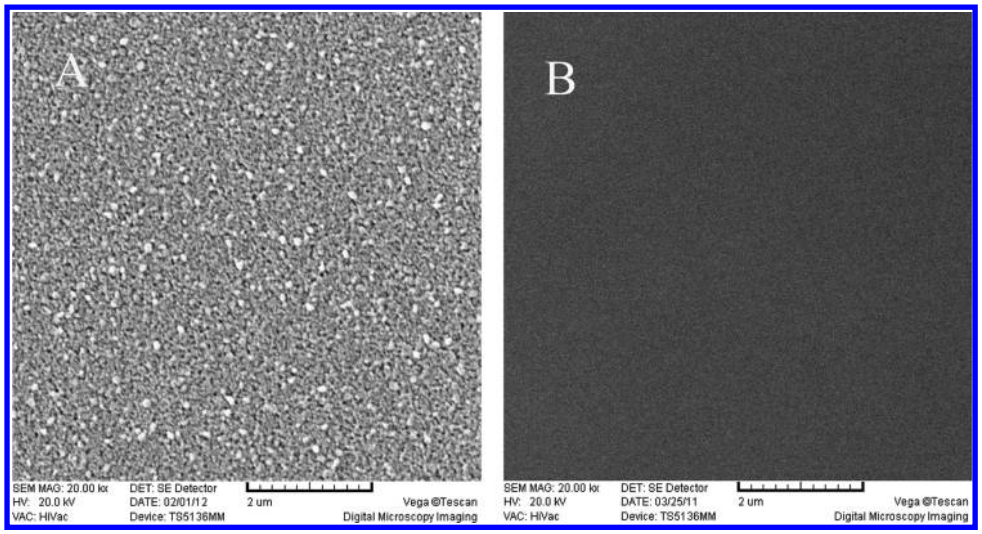

Figure 1. SEM images (×20 000) of (A) the neat WO_3 substrate and (B) the PT-WO_3 composite film.

Motivated by the ambition to create an active-layer material for the polymer solar cells, we here synthesize a new material consisting of WO_3 and polythiophene (PT). PT can exhibit a strong light-harvesting capacity under the sunlight due to its narrow bandgap (2.0 eV),[18,19] while WO_3 is known as one of versatile inorganic semiconductors and shows an excellent chemical stability, which allows it to survive harsh environments.[20] The optical and electrical properties of WO_3 highly depend on its crystal phases such as amorphous, triclinic, monoclinic, and hexagonal, which are sensitive to the preparing conditions.[21] It is important that as PT has the Lowest Unoccupied Molecular Orbital (LUMO) energy level higher than the WO_3 conduction band (CB) level, the energy difference makes possible the dissociation of photoexcited electron−hole pairs at the interface. PT intends to aggregate even in good solvents, but the semiconductor-initiated polymerization of this study permits this polymer to grow on the WO_3 substrate, leading to a uniform and high quality composite film. The polymer/nanocrystals interface which is produced from the special semiconductor-initiated polymerization is very interesting. Apart from the synthesis and photovoltaic properties of the PT-WO_3 composite film, the structures of the composite film are investigated with the aim of putting insight into the interface.

EXPERIMENTAL SECTION

Materials. Metallic tungsten powders (>99.99%), polyethylene oxide (PEO, M_w = 2 000 000) and Triton X-100 (polyoxyethylene isooctylphenyl ether) were purchased from Aldrich and used as received. Thiophene (Alfa Aesar, 99%) was distilled under passive vacuum before use. The Indium tin oxide (ITO) substrates (10 ohm/sheet, Shenzhen Nanbo Display Device Co., LTD) were carefully cleaned and dried by nitrogen. All other reagents were purified following common purification procedures.

Preparation of PT-WO_3 Film. WO_3 films were prepared using a sol−gel method. Triton X-100 was used as an additive to obtain uniform films. The sols were prepared according to the method proposed by Cronin et al.[22] Metallic tungsten was dissolved in a mixture of hydrogen peroxide (30%) and acetic acid at 0 °C for 24 h. The resulting solution was filtered then evaporated to dryness, resulting in a W-peroxy acid product. Subsequently, the product was reacted with ethanol at room temperature leading to W-peroxy ester sol. The ester sol was mixed with Triton X-100 (20% in volume). A few drops of the mixture were deposited onto an ITO substrate, and spun at an angular speed of 2000 rpm for 30s. All of the samples were dried in the air and annealed at different temperatures for 3 h.

The WO_3 film was placed upright in a quartz reactor which contains 100 mL of the thiophene aqueous suspension at 0.1 M. The thickness of the WO_3 substrate is 75 ± 10 nm unless otherwise indicated. The reactor was subjected to UV-irradiation at 365 nm for various lengths of time. The other reaction conditions were identical to those of our previous work.[10] The obtained hybrid films were rinsed with ethanol then dried by nitrogen. The control experiment with the thiophene aqueous suspension in absence of a WO_3 film showed that no polymer or oligomer was yielded under the identical reaction conditions, as determined by UV−vis spectroscopy, which is shown in the Supporting Information.

Characterization. Raman spectra were obtained with a LabRam-1B (Dilor) spectrometer. XPS was carried out with a PHI-5000C ESCA system (Perkin-Elmer) with Al Kα radiation. Atomic force microscope (AFM) of NanoScope IV and scanning electron microscope (SEM) of TS 5136MM were used to image surface morphologies of the films. The X-ray diffraction (XRD) pattern was recorded on a PANalytical X'Pert PRO (Cu Kα). UV−vis spectroscopy was obtained with a Lambda 35 spectrometer. Cyclic voltammetry experiments were performed using a Model 600A potentiostat/galvanostat (software CHI660) system. A platinum plate and a saturated calomel electrode (SCE) were used as counter and reference electrodes, respectively. The cyclic voltammetry curves were recorded in acetonitrile with $LiClO_4$ (0.5 M) as an electrolyte at a scan rate of 50 mV/s. The PT-WO_3 composite films were incorporated into thin-layer sandwich-type cells with Pt-coated counter electrodes and a gel-type electrolyte. The electrolyte was prepared by adding 5 wt % PEO into acetonitrile with lithium iodide (0.1 M) and iodine (0.05 M). IPCE action spectrum was measured using a Keithley 2400 high current source power meter at room temperature (298 K). Photocurrent measurements were taken using the Model 600A potentiostat/galvanostat (software CHI660) system under AM 1.5G white-light illumination from a 350 W xenon lamp.

RESULTS AND DISCUSSION

The structures of the annealed WO_3 films are gradually transformed from amorphous into monoclinic when the annealing temperature increases, as indicated by the XRD spectra (see Supporting Information). Among the WO_3 films obtained at different temperatures, the monoclinic WO_3 films obtained by annealing at 450 °C then slowly cooling to room temperature are found to have the best adhesion to the ITO substrate and be stable in the subsequent reactions. Therefore, the monoclinic films are selected as the initiators throughout

dx.doi.org/10.1021/la204990d | Langmuir 2012, 28, 4829−4834

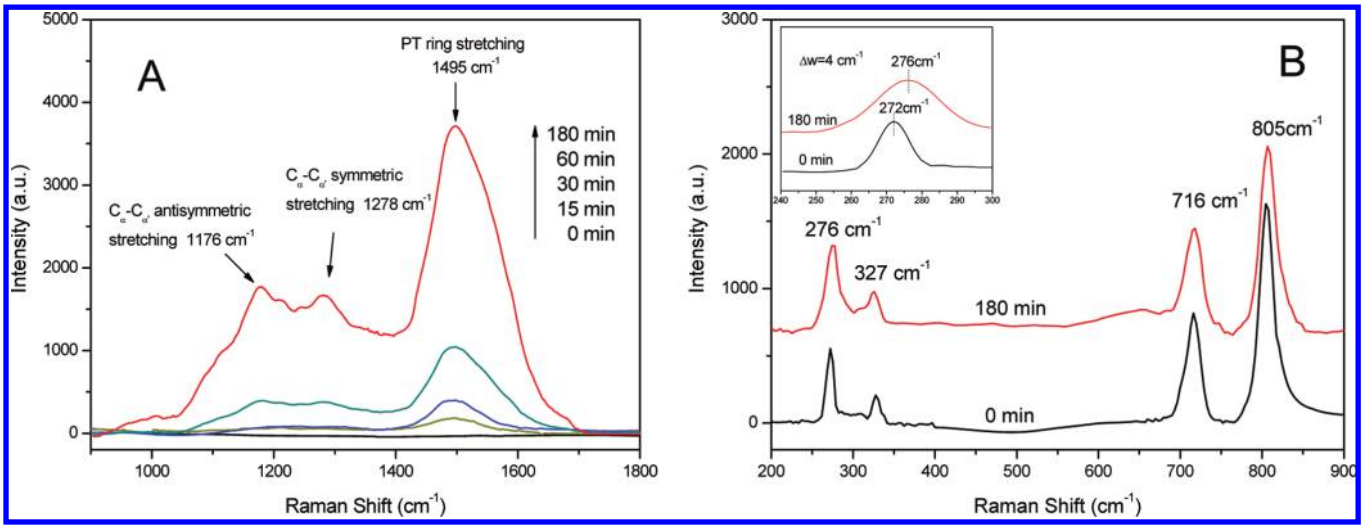

Figure 2. The Raman spectra in (A) polythiophene region and (B) WO_3 region versus the reaction time.

the experiments for preparing the composite films. Figure 1 compares the surface morphology of a reacted film with that of the neat WO_3 film. It is observed that the coarse WO_3 film is transformed to have a uniform surface as a result of the surface polymerization. According to the measure by the atomic force microscopy, the root-mean-square roughness (rms) of the surface decreases from 10.3 to 3.9 nm (see Supporting Information).

The synthesis of PT with the conjugated structure is proved by the Raman spectra plotted in Figure 2A, in which the most intense band centered at 1495 cm^{-1} is assigned to the stretching mode of thiophene rings of PT,[23] and the double peaks at 1278 and 1176 cm^{-1} are attributed to $C_\alpha-C_{\alpha'}$ symmetric and antisymmetric stretching of the backbone,[23] respectively. Figure 2B, which shows the spectral region of WO_3 confirms that the as-prepared WO_3 substrate has the typical monoclinic structure,[24] with the O−W−O bending vibrations of the bridging oxygen appearing at 276 and 327 cm^{-1} and the stretching vibrations at 716 and 805 cm^{-1}. Taking the strongest peak at 805 cm^{-1} as the internal standard, we obtain that the normalized intensity of the PT backbone stretching increases from 0 to 0.73 when the reaction lasts for 3 h. It is apparent that PT grows on the surface of the monoclinic WO_3 substrate with time. The thickness of the polymer layer is easy to control by the reaction time.

To evaluate the light-harvesting capacity of the PT-WO_3 composite film, the UV−vis absorption spectrum was measured and plotted in Figure 3. As observed in the spectrum, the PT component displays a broad absorption in the range from 450 to 750 nm, which originates from the photoexcited $\pi-\pi^*$ transitions.[25] The broad absorption band centered at 560 nm in Figure 3 originates from PT with a long chain length.[26] As for WO_3, it is interesting to observe that the absorption onset wavelength (λ_{onset}), which is a measure of bandgap, is shifted by 25 nm to a longer wavelength, as compared to the neat WO_3 substrate with λ_{onset} = 440 nm due to the bandgap 2.82 eV.[20] This result indicates that the WO_3 substrate exhibits a decrease of 0.15 eV in the bandgap as a result of the surface reaction and suggests an interaction in the composite film. In fact, the presence of the interaction is also implied by the Raman variation that the O−W−O bending band shows, a blue-shift in wavenumber and an obvious broadening in the fwhm (full-width at half-maximum), as illustrated in the inset to Figure 2B.

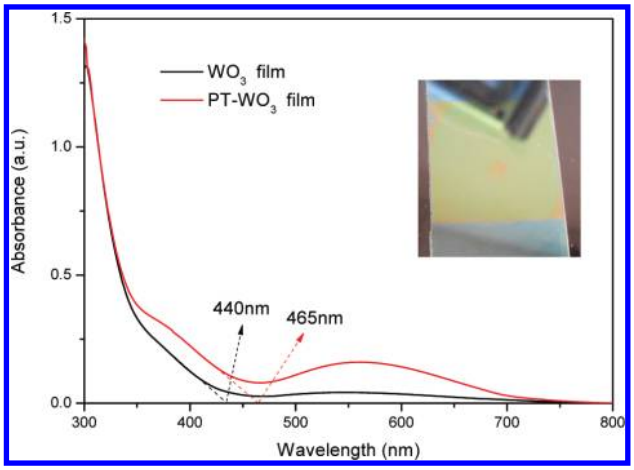

Figure 3. UV−vis spectra measured for the PT-WO_3 composite film and the neat WO_3 substrate. The photograph illustrates that the WO_3 substrate has a macroscopic uniform surface.

It is noteworthy that such Raman variations were detected in the sulfided tungsten oxides, which were considered to have covalent-like W−S−W and O−W−S bonds.[27,28] In our polymerization, it is necessary for WO_3 to interact with the thiophene monomers so that the initiation can proceed to the chain propagation. We carry out XPS and cyclic voltammetry analysis in the following studies in an attempt to establish the interface structure, which may provide information concerning the initiation reaction pathway.

It is found that the XPS W 4f core level shifts to a lower binding energy (BE), as illustrated in Figure 4A. This finding importantly reveals that the tungsten atoms participate in the interaction. By using the standard line-shape analysis, the W 4f spectrum is fitted with three components at 37.7, 36.0, and 34.6 eV, respectively. Typically, the first two components are assigned to the W(VI)[28] of the monoclinic WO_3. The component at the lowest energy indicates that part of tungsten atoms are reduced into the W(V) species, which usually appear at the binding energy near 34.6 eV.[28,29] As for the PT component, the S2p spectrum exclusive of the shoulder peak at 168.9 eV, as shown in Figure 4B, is characteristic of partly oxidized PT chains containing the aromatic unites (BE = 163.2 eV for S $2p_{3/2}$)[30] and the quinine moieties (BE = 164.9 eV for S

dx.doi.org/10.1021/la204990d | Langmuir 2012, 28, 4829−4834

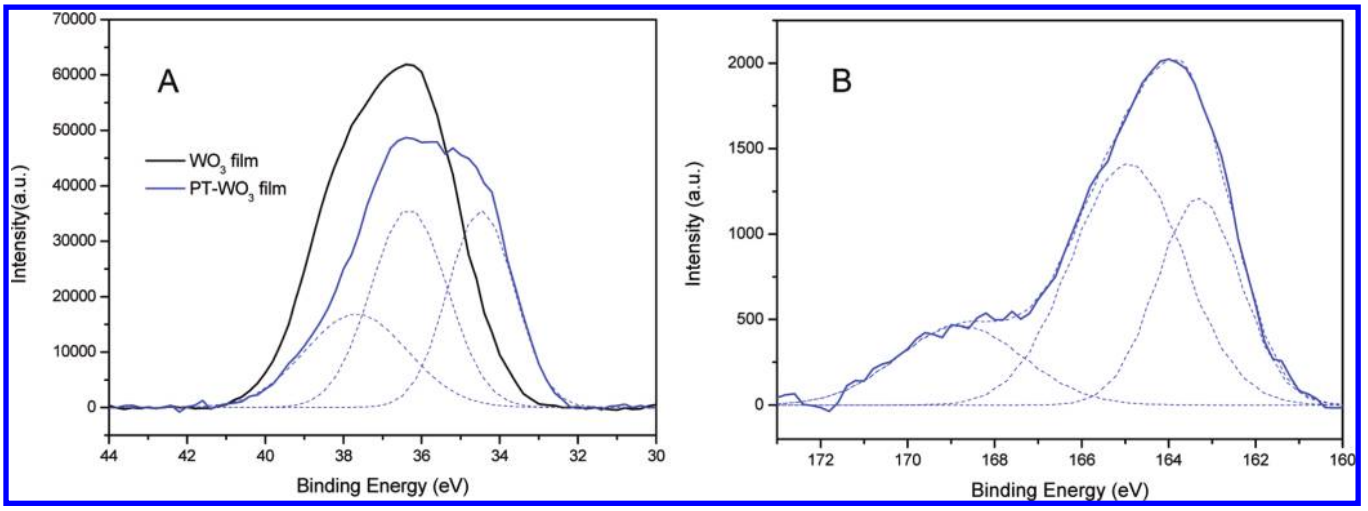

Figure 4. XPS spectra of (A) W 4f collected from the PT-WO_3 composite film and neat WO_3 substrate and (B) S 2p collected from the PT-WO_3 composite film.

$2p_{1/2}$)[30] of oxidized state. It is important that the newly occurring shoulder-peak at 168.9 eV is assigned to the positively charged sulfur ($S^{\delta+}$).[31] From the XPS results, it can be concluded that part of sulfur sites of PT are bound with the tungsten atoms in the substrate, probably leading to an acceptor−donor complex. Therefore, we put forward an interface structure as shown in Scheme 1 for the as-synthesized PT-WO_3 film. In this structure, the W(IV)−$S^{\delta+}$ bond at the interface is considered to originate from the special semiconductor-initiation.

Scheme 1. Illustration of the Interface between the Polythiophene Layer and WO_3 Substrate

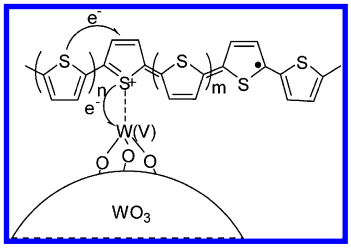

To obtain further information on the interface structure, the electrochemical analysis was carried out with the PT-WO_3 film. For comparison, Figure 5A gives the cyclic voltammetry of the neat WO_3 substrate in the liquid $LiClO_4$ electrolyte. As observed, the WO_3 substrate displays a cathodic reduction at the potential of about −1.5 V and an anodic oxidization occurring in the potential range of −0.8 to −0.3 V, dependent on the number of cycles. Figure 5B shows that the PT-WO_3 film exhibits a sequence of three cathodic peaks in the course of the negative scanning. It is observed that the PT-WO_3 film turns from olive green to dark blue when the voltage which is applied to the film exceeds −1.5 V vs SCE. The peak at −1.5 V is assigned to the WO_3, while both of the peaks at −0.45 and −0.98 V belong to the PT component. It is apparent that two distinct reduction reactions take place in the PT component. According to the peak sequences, the reductions appear to proceed in the steps by transferring electrons to the quinine moieties (as a result, the quinine structure is reduced to the aromatic one), subsequently to the positively charged sulfur, followed by the reduction of the W(IV) species at the interface.

In parallel to the above electronic processes, the ionic processes involving ion doping−undoping also take place due

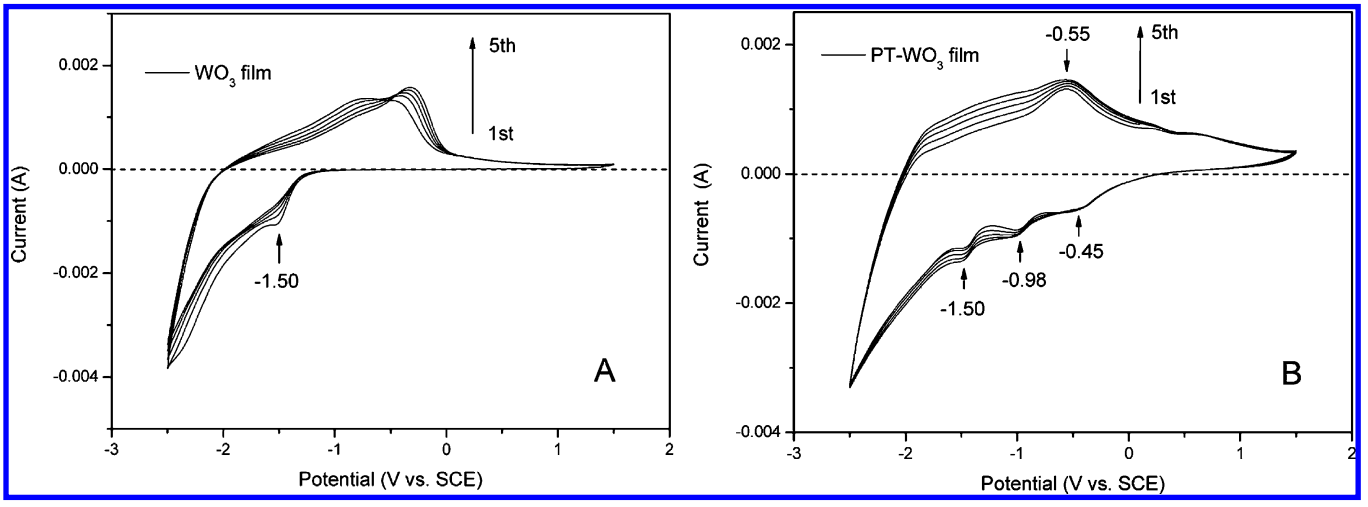

Figure 5. Cyclic voltammetry of (A) the neat WO_3 substrate and (B) the PT-WO_3 composite film.

dx.doi.org/10.1021/la204990d | *Langmuir* 2012, 28, 4829−4834

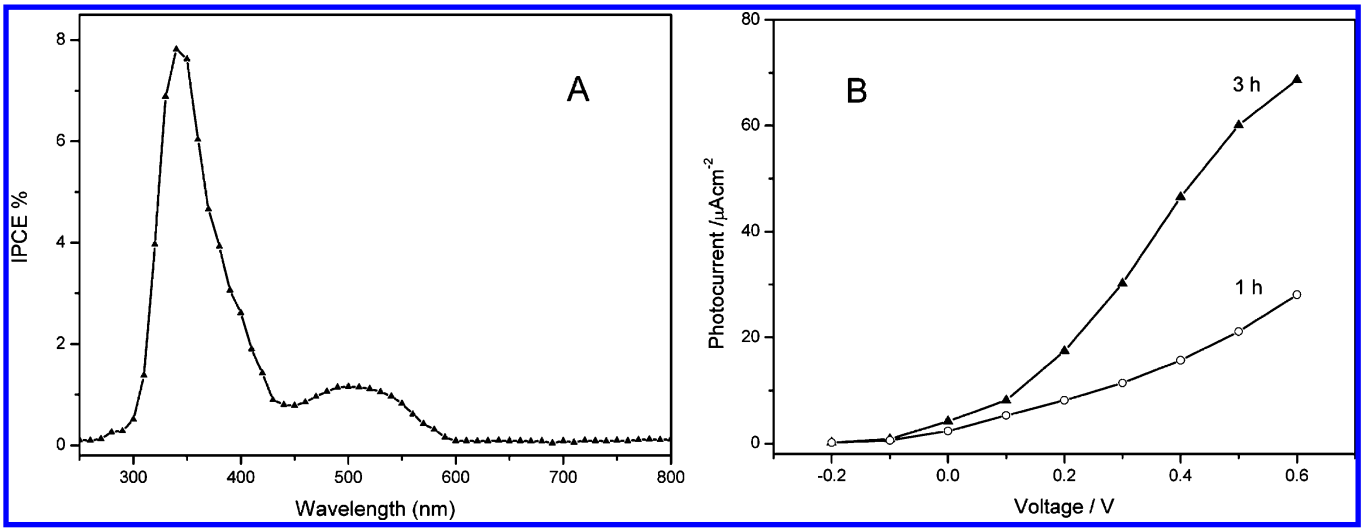

Figure 6. (A) IPCE action spectrum of the device fabricated from the PT-WO_3 composite film, which was obtained after 3 h reaction. The thickness of the WO_3 substrate here is 130 ± 15 nm. (B) Photocurrent characteristics of the PT-WO_3 composite films obtained after 1 and 3 h reaction.

to the electrolyte in contact. The shapes of the current−voltage response will be affected if the ionic processes are either irreversible or slow to recover.[32] The phenomenon that the anodic peak potential of the neat WO_3 is obviously shifted to higher ones with increasing the scanning cycles, as shown in Figure 5A, is attributed to the doping reaction of WO_3 with Li^+ ions.[33] In contrast, the WO_3 substrate in the composite film shows nearly the same anodic potential at −0.55 V, independent of the scanning cycles. This observation can be rationalized by the fact that the PT layer is dense and quickly bound to the substrate so that the WO_3 is kept away from the Li^+ doping.

The synthesized PT-WO_3 composite films are proven to have photovoltaic properties, as shown in Figure 6. As observed in the IPCE spectrum, which describes the relationship of photocurrent responses to incident photons, the PT-WO_3 film exhibits a sharp peak at 350 nm within the UV region and a broad band centered at 550 nm, which falls into the visible-light region. Comparing the IPCE spectrum with the absorption spectrum, which is plotted in Figure 3 reveals that both PT and WO_3 components are devoted to light-harvesting. The responses with a maximum efficiency of 8% within the UV region should be caused by the WO_3 light-harvesting, while the responses within the visible-light region are attributed to the PT light-harvesting. In the course of the incident sunlight penetrating across our film-device, the UV-light photons are captured by the WO_3 substrate due to its suitable bandgap, and the visible-light photons continue to penetrate toward the PT layer and are finally absorbed by the polymer. The electron−hole pairs, which are photogenerated from either WO_3 or PT are dissociated into free charge carriers at the interface, driven by the energy difference between the LUMO level of PT (−3.0 eV from vacuum)[34] and the CB level of WO_3 (−4.5 eV from vacuum).[35] The bond which links the WO_3 to PT probably offers an intramolecular charge transfer. We believe that the light-harvesting capacity of the PT layer depends on its thickness. To confirm this deduction, the photocurrent measurements were carried out on the composite films with different PT-layer thicknesses, which were controlled by the reaction time. The results show that the composite film obtained after 3 h reaction exhibits higher photocurrents than that of the film obtained after 1 h reaction. Although the photovoltaic performances of the devices at present are not satisfactory, the purpose of this study is to demonstrate that the semiconductor-initiated polymerization is an efficient approach to acquire the PT-WO_3 composite films having an intimately bound interface, which is a new candidate for solar cell materials. The devices are expected to show better photovoltaic performances when the device structures are optimized in respect of electron and hole transport.

■ CONCLUSIONS

A new photovoltaic hybrid film consisting of polythiophene and WO_3 has been synthesized by means of semiconductor-initiated polymerization. The polythiophene polymer continues to grow on the surface of the WO_3 substrate along with the reaction time. As a result, we obtain the PT-WO_3 composite films with a uniform surface. Analysis using XPS and cyclic voltammetry demonstrates that polythiophene is bound to WO_3 probably in the form of W−S bond and the acceptor−donor complex is generated at the interface as a result of the electron transfer from the polymer to WO_3. The device employing the PT-WO_3 film as the active-layer exhibits one IPCE peak at 350 nm and another peak at 550 nm. This study provides a new candidate for photovoltaic solar cell materials.

■ ASSOCIATED CONTENT

Supporting Information

X-ray diffraction data for the WO_3 films annealed at different temperatures. UV−vis absorption of thiophene aqueous suspension after UV irradiation. AFM topographies of the WO_3 film and the PT-WO_3 film. Schematic diagram of the energy levels of PT and WO_3. This material is available free of charge via the Internet at http://pubs.acs.org.

■ AUTHOR INFORMATION

Corresponding Author

*Tel: +86-21-65640982; fax: +86-21-65640293; e-mail: xyni@fudan.edu.cn.

Notes

The authors declare no competing financial interest.

■ ACKNOWLEDGMENTS

This work is supported by National Nature Science Foundation of China (NSFC) under Grant No. 20574011 and Shanghai Nanotechnology Promotion Center (SNPC) under Grant No. 1052 nm 01700.

■ REFERENCES

(1) Cheng, Y. J.; Yang, S. H.; Hsu, C. S. *Chem. Rev.* **2009**, *109*, 5868−5923.
(2) Guenes, S.; Neugebauer, H.; Sariciftci, N. S. *Chem. Rev.* **2007**, *107*, 1324−1338.
(3) Beek, W. J. E.; Wienk, M. M.; Kemerink, M.; Yang, X. N.; Janssen, R. A. J. *J. Phys. Chem. B* **2005**, *109*, 9505−9516.
(4) Huynh, W. U.; Dittmer, J. J.; Alivisatos, A. P. *Science* **2002**, *295*, 2426−2427.
(5) Liu, J. S.; Kadnikova, E. N.; Liu, Y. X.; McGehee, M. D.; Fréchet, J. M. J. *J. Am. Chem. Soc.* **2004**, *126*, 9486−9487.
(6) Arango, A. C.; Johnson, L. R.; Bliznyuk, V. N.; Schlesinger, Z.; Carter, S. A.; Hörhold, H.-H. *Adv. Mater.* **2000**, *12*, 1689−1692.
(7) Odoi, M. Y.; Hammer, N. I.; Sill, K.; Emrick, T.; Barnes, M. D. *J. Am. Chem. Soc.* **2006**, *128*, 3506−3507.
(8) Xu, J.; Wang, J.; Mitchell, M.; Mukherjee, P.; Jeffries-EL, M.; Petrich, J. W.; et al. *J. Am. Chem. Soc.* **2007**, *129*, 12828−12833.
(9) Liu, J. S.; Tanaka, T.; Sivula, K.; Alivisatos, A. P.; Frechet, J. M. J. *J. Am. Chem. Soc.* **2004**, *126*, 6550−6551.
(10) Weng, Z.; Ni, X. Y.; Yang, D. *J. Photochem. Photobiol. A: Chem.* **2009**, *201*, 151−156.
(11) Li, G. W.; Ni, X. Y. *J. Colloid Interface Sci.* **2009**, *334*, 8−12.
(12) Wang, J.; Ni, X. Y. *Solid State Commun.* **2008**, *146*, 239−244.
(13) Liu, X. F.; Ni, X. Y.; Wang, J. *Nanotechnology* **2008**, *19*, 485602−485607.
(14) Cheng, Y. J.; Hsien, C. H.; He, Y. J.; Hsu, C. S.; Li, Y. F. *J. Am. Chem. Soc.* **2010**, *132*, 17381−17383.
(15) Liao, H. H.; Chen, L. M.; Xu, Z.; Li, G.; Yang, Y. *Appl. Phys. Lett.* **2008**, *92*, 173303.
(16) Gur, I.; Fromer, N. A.; Chen, C. P.; Kanaras, A. G.; Alivisatos, A. P. *Nano Lett.* **2007**, *7*, 409−414.
(17) Saunders, B. R.; Turner, M. L. *Adv. Colloid Interface Sci.* **2008**, *138*, 1−23.
(18) Sanja, T.; Seth, B. D.; Nada, M. D.; Tijana, R.; Steven, J. S. *Small* **2009**, *5*, 1776−1783.
(19) Zade, S. S.; Bendikov, M. *Org. Lett.* **2006**, *8*, 5243−5246.
(20) Zheng, H. D.; Tachibana, Y.; Kalantar-zadeh, K. *Langmuir* **2010**, *26*, 19148−19152.
(21) Zheng, H. D.; Ou, J. Z.; Michael, S. S.; Richard, B. K.; Arnan, M.; Kalantar-zadeh., K. *Adv. Funct. Mater.* **2011**, *21*, 2175−2196.
(22) Cronin, J. P.; Tarico, D. J.; Agrawal, A.; Zhang, L. U.S. Patent 527986, 1992.
(23) Quoc, T. V.; Martin, P.; Niels, H.; Ursula, R.; Waldfried, P.; Jiri, P. *React. Funct. Polym.* **2005**, *65*, 69−77.
(24) Clara, S.; Marek, O.; Martine, U.; Jan, A. *J. Am. Chem. Soc.* **2001**, *123*, 10639−10649.
(25) Ong, B. S.; Wu, Y. L.; Liu, P.; Gardner, S. *Adv. Mater.* **2005**, *17*, 1141−1144.
(26) Jin, S.; Xue, G. *Macromolecules* **1997**, *30*, 5753−5757.
(27) Vlies, A. J. V.; Prins, R.; Weber, T. *J. Phys. Chem. B* **2002**, *106*, 9277−9285.
(28) Vlies, A. J. V.; Kishan, G.; Niemantsverdriet, J. W.; Prins, R.; Weber, T. *J. Phys. Chem. B* **2002**, *106*, 3449−3457.
(29) Le, Z.; Afanasiev, P.; Li, D. D.; Long, X. Y.; Vrinat, M. *Catal. Today* **2008**, *130*, 24−31.
(30) Han, Z. Y.; Zhang, J. C.; Yang, X. Y.; Zhu, H.; Cao, W. L. *Org. Electron.* **2010**, *11*, 1449−1460.
(31) Liang, H. C.; Li, X. Z. *Appl. Catal. B-Environ.* **2009**, *86*, 8−17.
(32) Levi, M. D.; Lopez, C.; Vieil, E.; Vorotyntsev., M. A. *Electrochim. Acta* **1997**, *42*, 757−769.
(33) Papaefthimiou, S.; Leftheriotis, G.; Yianoulis, P. *Electrochim. Acta* **2001**, *46*, 2145−2150.
(34) Jones, D.; Cuerra, M.; Favaretto, L. *J. Phys. Chem.* **1990**, *94*, 5761−5766.
(35) Grätzel, M. *Nature* **2001**, *414*, 338−344.